



# Molecular alignments in sexiphenyl thin films epitaxially grown on muscovite

H. Plank<sup>a</sup>, R. Resel<sup>a,\*</sup>, H. Sitter<sup>b</sup>, A. Andreev<sup>b</sup>, N.S. Sariciftci<sup>c</sup>, G. Hlawacek<sup>d</sup>, C. Teichert<sup>d</sup>,  
A. Thierry<sup>e</sup>, B. Lotz<sup>e</sup>

<sup>a</sup>*Institute of Solid State Physics, Graz University of Technology, Petersgasse 16, Graz 8010, Austria*

<sup>b</sup>*Institute for Semiconductor and Solid State Physics, University Linz, Altenberger Straße 69, Linz 4040, Austria*

<sup>c</sup>*Physical Chemistry, University Linz, Altenberger Straße 69, Linz 4040, Austria*

<sup>d</sup>*Institute of Physics, University Leoben, Franz Josef Straße 18, Leoben 8700, Austria*

<sup>e</sup>*Institute Charles Sadron, CNRS-UPR 22, 6, rue Boussingault, Strasbourg 67083, France*

Received 12 February 2003; received in revised form 23 June 2003; accepted 7 July 2003

## Abstract

The epitaxial orientations of highly crystalline para-sexiphenyl ( $C_{36}H_{26}$ ) films on mica (001) surfaces are investigated by selected area electron diffraction (SAED) and transmission electron microscopy (TEM). Films at the early growth stage (growth time 26 s) and at an advanced growth stage (growth time 10 min) are studied. Films at the early growth stage exhibit only three-dimensional islands with an average size of  $60 \times 30 \times 10 \text{ nm}^3$ , whereas films at an advanced growth stage consist of long oriented nano-fibres with a needle-like morphology. We identified three different types of epitaxial relations between the mica (001) substrate and the sexiphenyl crystallites, which are the same in both growth stages. Moreover, within a single island as well as within a single fibre crystalline domains with these three epitaxial orientations are observed. At the advanced growth stage, these domains are aligned antiparallel or perpendicular to the fibre axes; the typical size of the domains is 20 nm.

© 2003 Elsevier B.V. All rights reserved.

PACS: 68.37.-d; 68.37.Lp; 61.14.-x; 72.80.Le; 81.10.-h

Keywords: Epitaxy; Grain boundary; Electron diffraction; Organic semiconductors

## 1. Introduction

During the last decade the conjugated organic semiconductor para-sexiphenyl ( $C_{36}H_{26}$ , PSP) has attracted much interest for applications in opto-electronics such as light emitting devices, field effect transistors (FET), solar cells, a.o [1–5]. In all these applications PSP is used as a polycrystalline thin film supported by a substrate. The preferred orientation of the molecules relative to the substrate influences the device performance, since the electronic and optical properties of the thin films are highly anisotropic [4,5]. The crystallite size is another important parameter for successful device operation as shown in FET's fabricated from sexithophene [6]. Moreover, it was shown that organic single

crystal devices show a markedly enhanced performance, since the electronic transport in monocrystalline structures is not hindered by grain boundaries [7]. Obviously, control of the growth of organic molecules on single crystal surfaces is needed for a further improvement in the device performance [8]. The molecular orientation relative to the substrate and the size of the monocrystalline domains can be controlled to a certain extent by epitaxial growth conditions.

Recently, it was shown that PSP grows in a highly ordered fashion on a mica (001) surface, resulting in long (up to the mm range) nano-fibres, which are oriented parallel to each other [9–11]. Such structures show high optical anisotropy with dichroic ratios of more than 11 [9]. Previous X-ray diffraction (XRD) studies indicated that the  $\beta$ -phase of PSP is present within these films [12]. Three different epitaxial relationships between the mica substrate and PSP crystallites

\*Corresponding author. Tel.: +43-316-873-847; fax: +43-316-873-84786.

E-mail address: [roland.resel@tugraz.at](mailto:roland.resel@tugraz.at) (R. Resel).

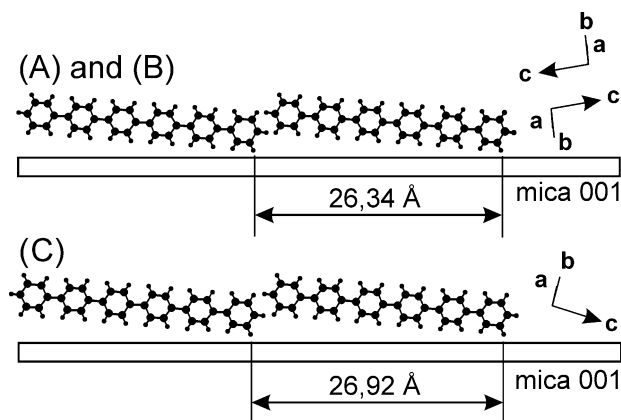


Fig. 1. Side view of sexiphenyl molecules relative to the mica (001) substrate as they are oriented within their epitaxial orientations. Top part: orientations (A) and (B) with the same intermolecular distance of  $a=26.34$  Å. Bottom part: orientation (C) with another  $a=26.92$  Å. For each of these three orientations the unit cell vectors of epitaxially grown sexiphenyl are given at the right side.

were observed in very thick films:  $(11-1)_{\text{PSP}}\parallel(001)_{\text{mica}}$  and  $[1-2-1]_{\text{PSP}}\parallel[-340]_{\text{mica}}$  (orientation (A));  $(-1-11)_{\text{PSP}}\parallel(001)_{\text{mica}}$  and  $[-110]_{\text{PSP}}\parallel[-340]_{\text{mica}}$  (orientation (B)) and  $(11-2)_{\text{PSP}}\parallel(001)_{\text{mica}}$  and  $[-20-1]_{\text{PSP}}\parallel[-310]_{\text{mica}}$  (orientation (C)) [13]. These three orientations of the molecules relative to the substrate are shown in Fig. 1. In all three cases the alignment of the long molecular axes is approximately in the same. To visualize the differences of the three orientations, the different directions of the unit cell vectors are given. As reported in Ref. [13], PSP grows on mica (001) in an incommensurate mode. Nevertheless, a high degree of epitaxial alignment was observed by rocking curves with a FWHM as low as  $0.062^\circ$  [14].

The above mentioned results were obtained from rather thick films. Note, that in this case XRD provided us only integral information over the whole area of the X-ray spot and the thickness of the film. However, to understand the growth manner of such nano-fibres, much thinner films had to be investigated with high local resolution. The aim of this paper is a detailed investigation of thin PSP films grown on mica (001) using selected area electron diffraction (SAED) and transmission electron microscopy (TEM) techniques.

## 2. Experimental techniques

The thin PSP films were prepared by Hot Wall Epitaxy on freshly cleaved single crystalline muscovite (mica) substrates [9,15]. Mica crystallize in a monoclinic structure with lattice constants of  $a=5.20$  Å,  $b=9.03$  Å,  $c=20.11$  Å and  $\beta=95.78^\circ$ ; the easy accessible cleavage plane corresponds to (001) [16]. The vacuum during growth was approximately  $6\times 10^{-6}$  mbar, the PSP source temperature was  $240^\circ\text{C}$  and the substrate

temperature was fixed at  $90^\circ\text{C}$ . Based on the results of Ref. [17] we selected two deposition times in order to investigate and compare qualitatively different growth stages of PSP on mica (001): 26 s (corresponding to early growth stage) and 10 min (advanced growth stage), resulting in an average film thickness of 1 and 20 nm, respectively. Further growth details can be found in [9].

The preparation of the PSP films for TEM/SAED (transmission electron microscopy/selected area electron diffraction) investigations starts with the deposition of a thin carbon film. The carbon film stabilizes the PSP film after removing from the mica substrate and helps to avoid sample charging by the electron beam. Subsequently, the PSP/carbon film is removed from the substrate with hydrofluoric acid (HF) (5 wt.% solution in water). The film fragments floating on the HF surface are picked onto copper grids. SAED/TEM investigations are performed with a Philips CM 12 electron microscope at energy of 120 keV. The diffraction patterns are taken by focussing the beam spot to diameters ranging from  $20\ \mu\text{m}$  down to  $0.1\ \mu\text{m}$ . The images are recorded on AGFA Scientia EM films. In order to determine the investigated area of the sample from which the SAED pattern was taken, the pattern was slightly defocused and the investigated area appears as shaded region within the resulting image. Unfortunately, no scale can be given for the defocused SAED images. The given dimensions of the islands (for the sample grown for 26 s) are evaluated from scaled TEM images. Dark field images were taken from the samples by tilting the primary electron beam.

Indexation of the experimental diffraction pattern was carried out with the software Cerius by ACCELRYs based on the  $\beta$ -phase of PSP [12]. Bulk PSP crystallizes in a monoclinic lattice with  $a=8.091$  Å,  $b=5.565$  Å,  $c=26.24$  Å and  $\beta=98.17^\circ$ . The arrangements of the PSP molecules relative to each other and relative to the substrate are carried out on the basis of single crystal data; the graphical representations are taken from the crystallographic software POWDER CELL [18].

Atomic force microscopy investigations (AFM) were performed with a Digital Instruments Multimode IIIa microscope in tapping mode. High-density carbon tips in combination with low tip velocity were used for high-resolution imaging; the frequency of the cantilever was 316 Hz, the scan rate was  $2.8\ \mu\text{m/s}$ .

## 3. Experimental results

In Fig. 2 SAED results are presented for the advanced growth stage. Fig. 2a shows the TEM morphology typical for this growth stage representing long nano-fibres. This result is in qualitative agreement with previous AFM investigations [17]. The fibres are partly interrupted, they have still different widths, branching

of the fibres is observed occasionally. In nearly all cases the length of the fibres exceeds the size of the imaged area. Two typical types of diffraction pattern of the sample are shown in Fig. 2b,c; the patterns were taken from different areas including a large number of fibres. The assignment of the diffraction patterns to the orientation of the nanofibres is not given here, but published elsewhere [13]. The diffraction spots in Fig. 2b are aligned in rows parallel to the meridian (direction along the  $00l$  diffraction spots). The other diffraction spot parallel to the meridian corresponds to PSP  $-21l$  on one side and  $2-1-l$  on the other. However, we see two rows of  $00l$  spots at the meridian, which are tilted by an angle of  $\sim 5^\circ$ . This tilt angle is also present for  $21l$  rows, and as a consequence they are not clearly separated from each other: the  $-213$  and  $2-1-3$  are smeared out due to overlapping of strong diffraction spots. These two sets of diffraction spots indicate the presence of two slightly different orientations of the crystallites corresponding to orientation (A) and (B), since the  $(001)$  plane of PSP crystallites in orientations (A) and (B) are tilted by  $5^\circ$ . Also, in Fig. 2c two sets of  $(00l)$  diffraction spots are present along the meridian, these two rows are tilted by  $16^\circ$ . They correspond to orientations (A) and (C). Selected area diffraction as well as extensive dark field investigations performed on a part of an individual fibre reveals that two or sometimes all three orientations are present within the single fibre. Two typical dark field images are shown in Fig. 3. These images were taken from the elongated  $-213$  reflections of individual PSP fibres. Dark and light areas are clearly visible; those areas are either perpendicular (left part) or parallel to the fibre axis (right part). In this negative image, the dark and light areas are due to Bragg contrast. The typical width indicated by the contrast is approximately 20 nm. A clear identification of the individual orientations cannot be obtained, since the  $-213$  diffraction peaks is smeared out (as described above) so that this reflection cannot be clearly isolated

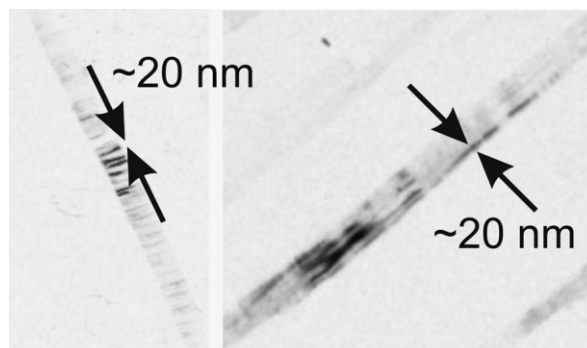


Fig. 3. Dark field images taken from  $-213$  reflections, from two different PSP fibres. The ordered domains are arranged in a stripe like structures, which are all parallel to the fibres axis (right side) or perpendicular to that (left side). The typical width of the domains is approximately 20 nm, which is revealed by the Bragg contrast (dark fringes).

for each orientation [19]. These experimental results give the clear evidence that even one single nano-fibre of sexiphenyl does not represent a single crystalline domain; a frequent change from one crystalline orientation to another appears.

In order to understand the origin of the three orientations (A), (B) and (C), found in the single fibres, the films grown in the early stage of deposition were also investigated by SAED/TEM. Based on the data of Ref. [17] we chose the growth time of 26 s, since it results in an island type morphology. Fig. 4a shows the morphology of this film taken using defocused SAED. As expected, this result is in good agreement with previous AFM investigations [17]. Taken from a real TEM image of the same film, the typical dimensions of the islands are determined at: 60 nm in length and 30 nm in width with an area density of  $12 \mu\text{m}^{-2}$ . A diffraction pattern taken from a large number of islands is shown in Fig. 4b and a zoom of the diffraction pattern along the meridian direction in Fig. 4c. A hint for the presence of

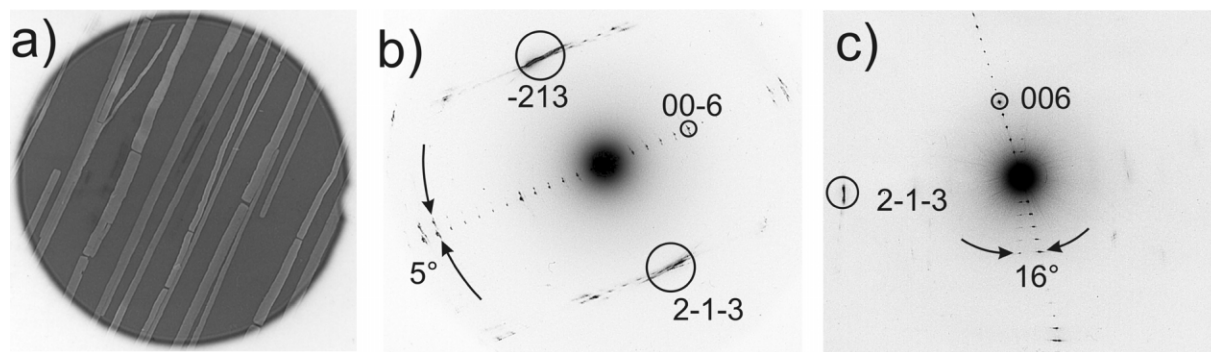


Fig. 2. (a) Typical defocused SAED image of the PSP nano-fibres; (b) a SAED pattern from crystallites of orientation (A) and (B); (c) SAED pattern from crystallites with orientation (A) and (C). Along the meridian only the  $006$  and  $00-6$  reflections are indexed. Note, no absolute scale can be given in (a) because the image was taken in defocused mode.

different orientations of the PSP crystallites is the smeared -213 reflection (circled). Along the meridian, the 006 reflection is split in three components. Around the centre of the diffraction pattern they tilt  $5^\circ$  and  $16^\circ$  away from each other (Fig. 4c). This observation reveals the presence of all three orientations (A), (B) and (C) already in the early growth stage of the film. The diffraction pattern taken from a single island is shown in Fig. 5 together with the corresponding defocused image. The dark spot in the defocused image marks the individual island from which the diffraction pattern was taken. In this case, two sets of diffraction spots are present. The smeared -213 reflections as well as the characteristic  $16^\circ$  tilt of the 006 reflections along the meridian (described previously) can be identified. This observation demonstrates that already in a small single island more than one epitaxial orientation is present.

#### 4. Discussion

As in all types of epitaxial crystallisation, the contact plane of the deposit corresponds to a cleavage plane. The unexpected feature for PSP on mica (001) is that diffraction and dark field electron microscopy clearly indicate that three different orientation co-exists, that corresponds to three different contact (cleavage) planes. The cleavage planes are (11-1) for orientation (A), (-1-11) for (B) and (11-2) for (C). This diversity implies that the interactions between the PSP molecules (within the bulk) are important for the development of specific orientations of the crystallites relative to the substrate. However, the PSP crystallites are aligned along specific directions on the mica (001) surface: in case of (A)  $[1-21]_{\text{PSP}}\parallel[-340]_{\text{mica}}$ , for (B)  $[-110]_{\text{PSP}}\parallel[-340]_{\text{mica}}$  and for (C)  $[-201]_{\text{PSP}}\parallel[-310]_{\text{mica}}$ . That means

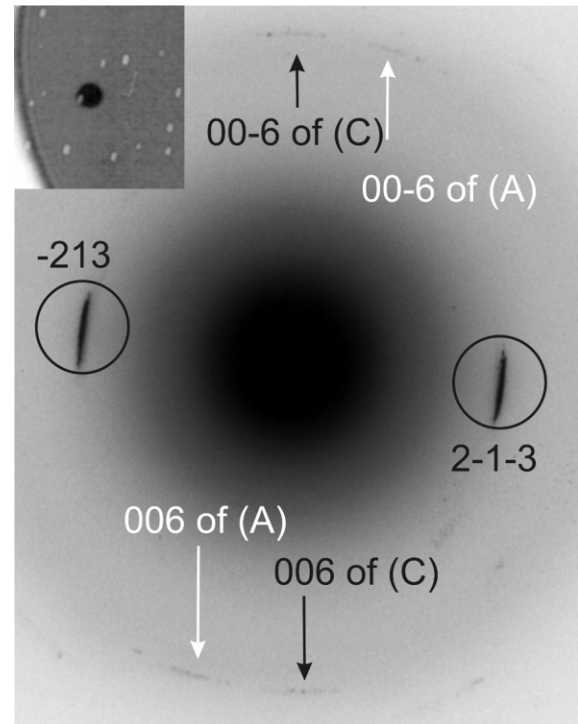


Fig. 5. SAED pattern from a single island indicating two crystal orientations within the island. The inset is a defocused diffraction image showing the individual island from which the SAED pattern was taken.

that the weak interactions of the PSP molecules with the mica (001) surface under HWE conditions are strong enough to introduce epitaxial orientations in PSP crystallites [11,13,20]. Moreover, our results demonstrate that both (above mentioned) types of interactions are responsible for the formation of epitaxial order as

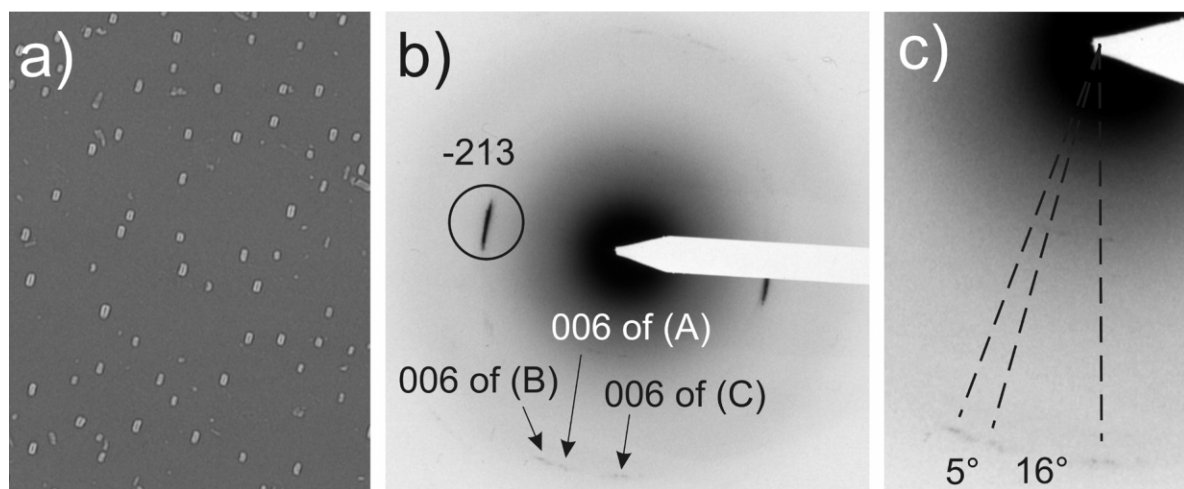


Fig. 4. (a) Typical defocused SAED image of a sample grown for 26 s. The island type morphology is clearly visible. (b) The SAED pattern reveals clearly the presence of three different orientations, (c) enlargement of (b) along the meridian with the indication of characteristic angles between the three sets of diffraction spots. Note, no absolute scale can be given in (a) because the image was taken in defocused mode.

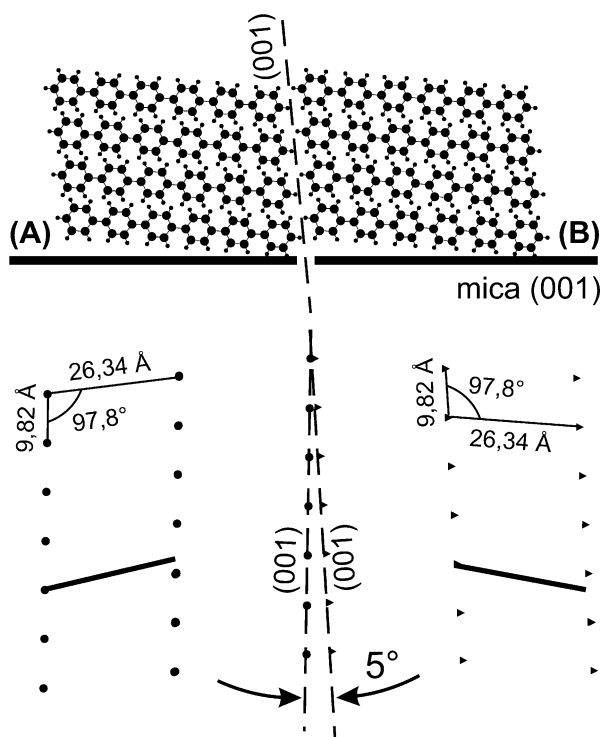


Fig. 6. Side view and top view of the alignment of the PSP molecules for the transition from orientation (A) (left side) to (B) (right side). In the top view (below) the two-dimensional lattice is given by filled circles for orientation (A) and by triangles for orientation (B). The two short thick lines indicate the alignment of the long axis of PSP molecules for (A) and (B).

discussed also for other organic molecules grown on inorganic substrates [21–25]. Note, from our observations we cannot make any conclusions about the orientation of the molecules within the first monolayers. Therefore, it is conceivable that for a few first layers of PSP on mica the molecular orientations are different from ones described above. Moreover, it is known that in epitaxially grown organic films considerable differences between the arrangements of the molecules within the first layers and the bulk crystallites can be present [26,27].

A second important observation is that within a single fibre as well as an individual island more than one orientation is found. The co-existence of different orientations within the bulk is analysed by the arrangement of the molecules along particular crystallographic planes. The (001) plane of PSP would be a perfect twinning plane, which would enable the transition from one orientation to another, as shown in Fig. 6 for the transition from (A) to (B). The upper part of Fig. 6 shows a side view of the molecules in orientation (A) on the left side and the orientation (B) on the right side. The twinning plane is indicated by the dashed line between (A) and (B). The lower part of the figure shows a top view of the two-dimensional lattices of (A)

(filled circles) and of (B) (triangles). These lattices are generated by the two two-dimensional periodicity of the crystallographic plane of PSP, which is parallel to the mica (001) surface (e.g. (11-1) for orientation (A)). In case of orientation (A) and (B) the unit cell of the two-dimensional lattices are given as:  $a=26.34$  Å,  $b=9.82$  Å and  $\alpha=97.8^\circ$  and for (C)  $a=26.92$  Å,  $b=9.82$  Å and  $\alpha=91.0^\circ$  [13], as indicated in Fig. 6. One can see that the perfect twinning is not observed, since the (001) planes for (A) and (B) are not fully parallel to each other—a tilt angle of approximately  $5^\circ$  is observed between them. The short thick lines represent the alignment of PSP molecules (in direction of the long molecular axes) relative to the two-dimensional lattice. One can see that the (001) plane is aligned perpendicular to the molecules (also parallel to the fibres axis [9]). Therefore, the boundaries of two PSP domains are in the same direction along the fibre axis, which is in a good agreement with our dark field observations (Fig. 3).

Another possible twinning plane is (-213) as shown in Fig. 7 for a transition from (B) to (C). In the upper part of the figure a projection parallel to the mica substrate along the long molecular axes is depicted for the orientation (B) on the left side and for orientation (C) on the right side. The twinning plane is indicated

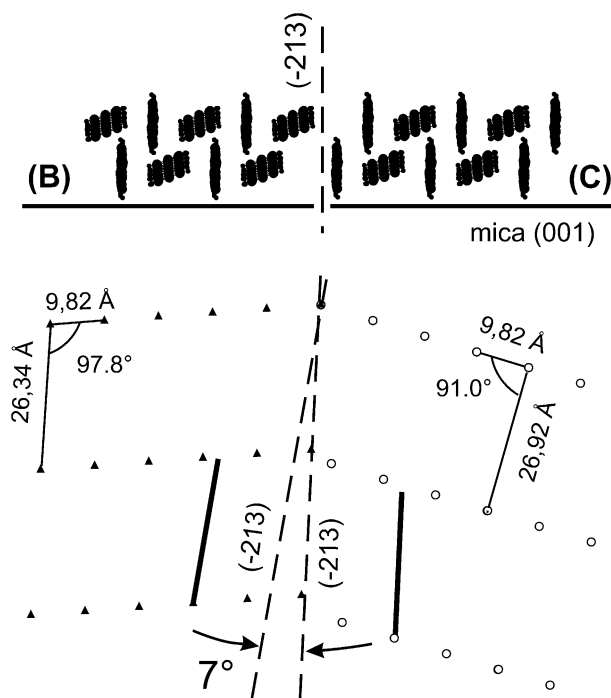


Fig. 7. Parallel view and top view of the alignment of the PSP molecules for the transition from orientation (B) (left side) to orientation (C) (right side). In the top view (below) the two-dimensional lattice is given by triangles for (B) and by open circles for (C) orientation. The (-213) planes of PSP are drawn by dashed lines. The thick lines represent the long axis of PSP molecules.

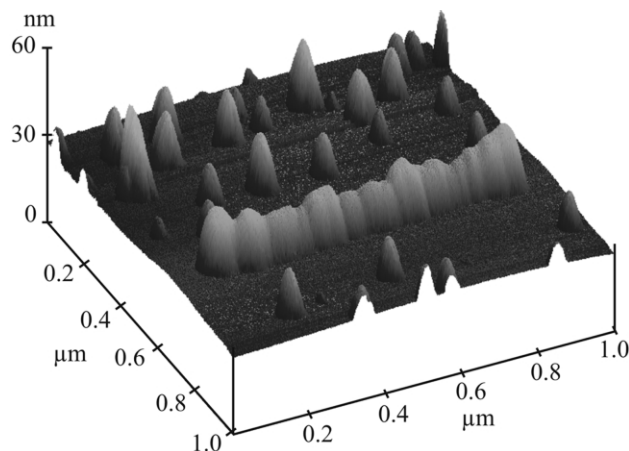


Fig. 8. Three-dimensional AFM image showing individual PSP islands as well as a well-oriented nanofibre. Please note that the vertical scale is exaggerated by a factor of approximately 8.

between the two orientations by a dashed line. We see that in this case, the twinning is also not perfect, since the (-213) plane of (B) and the (-213) plane of (C) are tilted by an angle of  $7^\circ$  relative to each other. In the lower part of the figure the two-dimensional lattice for (B) and (C) are drawn by triangles and open circles, respectively. The (-213) planes are depicted for both orientations by dashed lines and PSP molecules are indicated for both orientations by thick lines. One can see that in this model the boundaries between PSP domains are perpendicular to the fibre axis, which is again in agreement with ‘perpendicular’ domains observed in dark field experiments (Fig. 3).

The co-existence of different epitaxial orientations even within an individual island cannot be explained by a simple model of ‘perfect’ or ‘geometric’ twinning. However, we clearly observe the arrangement of the crystalline domains with different orientations approximately along their cleavage planes. That means that another mechanism (not twinning) is responsible for this effect. Probably, the growth kinetic effects like coalescence of small migrating islands can solve the puzzle. This assumption is supported by recent atomic force microscopy studies (AFM), which was performed in dependence on the growth time. Fig. 8 shows a high-resolution AFM image of the early growth stage (deposition time: 35 s). The image reveals the coexistence of individual islands and nanofibres. The islands have an average height of 17 nm, and a footprint of approximately  $50 \times 100$  nm. In the image of the roughly 850 nm long fibre approximately 15 of such individual islands can be resolved. This result strongly indicates that long nanofibres of PSP on mica are formed by regrouping of small individual islands originating from earlier growth stages. Further investigations concerning

the formation of such fibres and their structure are in progress.

Summarized, the needle-like morphology in the advanced growth stage is composed of small individual domains which have a size of approximately 20 nm. This size is comparable with the island size at the early growth stage where island type morphology with dimensions of  $60 \times 30 \times 10$  nm in length, width and height is observed. The linking of the individual domains with different epitaxial orientation to a continuously packed bulk cannot be fully explained by a simple model of ‘geometric’ twinning. In principle, the crystallographic planes (001) and (-213) would suit as twinning planes. But, for different epitaxial orientations these planes are not absolutely parallel to each other, a shift of few degrees is observed. Therefore, the geometric requirements for the formation of reflection twins are not fully achieved.

## 5. Conclusions

SAED investigations on thin PSP films epitaxially grown on mica (001) reveal full agreement with previous XRD results performed for thick films. The same types of orientations are observed at the early growth stage (islands morphology) as well as at an advanced stage (nano-fibers morphology). These facts suggest that the crystalline structure of the films remains nearly identical in the whole range of the film thicknesses investigated. Moreover, these orientations co-exist even within a single fibre as well as within an individual island, which leads to the formation of different crystalline domains. Dark field investigations reveal the existence of highly ordered PSP domains of approximately 20 nm width oriented parallel and perpendicular to the long PSP nano-fibres.

## Acknowledgments

This work was supported by the RTN-Network EUROFET and by the Austrian Science Foundation (projects P15626 and P15155).

## References

- [1] S. Tasch, C. Brandstätter, F. Meghdadi, G. Leising, G. Froyer, L. Athouel, *Adv. Mater.* 9 (1997) 33.
- [2] D.J. Gundlach, Y.-Y. Lin, T.N. Jackson, D.G. Schlom, *Appl. Phys. Lett.* 71 (1997) 3853.
- [3] G. Meinhardt, W. Graupner, G. Feistritzer, R. Schröder, E.J.W. List, A. Pogantsch, G. Dicker, B. Schlicke, N. Schulte, A.D. Schlüter, G. Winter, M. Hanack, U. Scherf, K. Müllen, G. Leising, *Proc. SPIE* 3623 (1999) 46.
- [4] T. Mikami, H. Yanagi, *Appl. Phys. Lett.* 73 (1998) 563.
- [5] H. Yanagi, S. Okamoto, *Appl. Phys. Lett.* 71 (1997) 2565.
- [6] G. Horowitz, M.E. Hajlaoui, *Adv. Mater.* 12 (2000) 1046.
- [7] G. Horowitz, F. Garnier, A. Yassar, R. Hajlaoui, F. Kouki, *Adv. Mater.* 8 (1996) 52.

- [8] S.R. Forrest, *Chem. Rev.* 97 (1997) 1793.
- [9] A. Andreev, G. Matt, C.J. Brabec, H. Sitter, D. Badt, H. Seyringer, N.S. Sariciftci, *Adv. Mater.* 12 (2000) 629.
- [10] F. Balzer, H.G. Rubahn, *Appl. Phys. Lett.* 79 (2001) 3860.
- [11] F. Balzer, H.G. Rubahn, *Surf. Sci.* 507–511 (2002) 588.
- [12] K.N. Baker, A.V. Fratini, T. Resch, H.C. Knachel, W.W. Adams, E.P. Socci, B.L. Farmer, *Polymer* 34 (1993) 1571.
- [13] H. Plank, R. Resel, S. Purger, J. Keckes, A. Thierry, B. Lotz, A. Andreev, N.S. Sariciftci, H. Sitter, *Phys. Rev. B* 64 (2001) 235 423.
- [14] A. Andreev, H. Sitter, R. Resel, D.M. Smilgies, H. Hoppe, G. Matt, N.S. Sariciftci, D. Meissner, D. Lysacek, L. Valek, *Mol. Cryst. Liq. Cryst.* 385 (2002) 61.
- [15] A. Lopez-Otero, *Thin Solid Films* 49 (1978) 3.
- [16] S.W. Bailey. in: Brindley G.W., Brown G. (Eds.), *Crystal Structure of Clay Minerals and their X-ray Identification*, Mineral Society Monograph 5, London, 1980, 1.
- [17] A. Andreev, H. Sitter, C.J. Brabec, P. Hinterdorfer, G. Springholz, N.S. Sariciftci, *Synth. Met.* 121 (2001) 1379.
- [18] W. Kraus, G. Nolze, *J. Appl. Cryst.* 29 (1996) 301.
- [19] H. Plank, Diploma Thesis Graz University of Technology 2002.
- [20] H. Plank, R. Resel, A. Andreev, N.S. Sariciftci, H. Sitter, *J. Cryst. Growth* 237–239 (2002) 2076.
- [21] E. Umbach, K. Glöckler, M. Sokolowski, *Surf. Sci.* 402–404 (1998) 20.
- [22] C. Ludwig, B. Gompf, W. Glatz, J. Petersen, W. Eisenmenger, M. Möbus, U. Zimmermann, N. Karl, *Z. Phys.* B86 (1992) 397.
- [23] S.R. Forrest, Y. Zhang, *Phys. Rev. B* 49 (1994) 11 297.
- [24] A. Richter, R. Ries, K. Szulzewsky, B. Pietzak, R. Smith, *Surf. Sci.* 394 (1997) 201.
- [25] F. Biscarini, R. Zamboni, P. Samori, P. Ostojca, C. Taliani, *Phys. Rev. B* 52 (1995) 14 868.
- [26] Z. Wu, S.N. Ehrlich, B. Matthies, K.W. Herwig, P. Dai, U.G. Vilkmann, F.Y. Hansen, H. Taub, *Chem. Phys. Lett.* 348 (2001) 168.
- [27] K.W. Herwig, J.C. Newton, H. Taub, *Phys. Rev. B* 50 (1994) 15 287.